Measurement of W-Boson Production in 1.8-TeV $\bar{p}p$ Collisions

F. Abe,[8] D. Amidei,[3] G. Apollinari,[11] G. Ascoli,[7] M. Atac,[4] P. Auchincloss,[14] A. R. Baden,[6] A. Barbaro-Galtieri,[9] V. E. Barnes,[12] F. Bedeschi,[11] S. Belforte,[11] G. Bellettini,[11] J. Bellinger,[17] J. Bensinger,[2] A. Beretvas,[14] P. Berge,[4] S. Bertolucci,[5] S. Bhadra,[7] M. Binkley,[4] R. Blair,[1] C. Blocker,[2] J. Bofill,[4] A. W. Booth,[4] G. Brandenburg,[6] D. Brown,[6] A. Byon,[12] K. L. Byrum,[17] M. Campbell,[3] R. Carey,[6] W. Carithers,[9] D. Carlsmith,[17] J. T. Carroll,[4] R. Cashmore,[4] F. Cervelli,[11] K. Chadwick,[4,12] T. Chapin,[13] G. Chiarelli,[11] W. Chinowsky,[9] S. Cihangir,[15] A. Clark,[4] D. Cline,[17] D. Connor,[10] M. Contreras,[2] J. Cooper,[4] M. Cordelli,[5] M. Cuatolo,[5] C. Day,[4] R. DelFabbro,[11] M. Dell'Orso,[11] L. DeMortier,[2] T. Devlin,[14] D. DiBitonto,[15] R. Diebold,[1] F. Dittus,[4] A. DiVirgilio,[11] J. E. Elias,[4] R. Ely,[9] S. Errede,[7] B. Esposito,[5] B. Flaugher,[14] E. Focardi,[11] G. W. Foster,[4] M. Franklin,[6,7] J. Freeman,[4] H. Frisch,[3] Y. Fukui,[8] A. F. Garfinkel,[12] P. Giannetti,[11] N. Giokaris,[13] P. Giromini,[5] L. Gladney,[10] M. Gold,[9] K. Goulianos,[13] C. Grosso-Pilcher,[3] C. Haber,[9] S. R. Hahn,[10] R. Handler,[17] R. M. Harris,[9] J. Hauser,[3] T. Hessing,[15] Y. Hayashide,[16] R. Hollebeek,[10] L. Holloway,[7] P. Hu,[14] B. Hubbard,[9] P. Hurst,[7] J. Huth,[4] H. Jensen,[4] R. P. Johnson,[4] U. Joshi,[14] R. W. Kadel,[4] T. Kamon,[15] S. Kanda,[16] D. Kardelis,[7] I. Karliner,[7] E. Kearns,[6] R. Kephart,[4] P. Kesten,[2] H. Keutelian,[7] S. Kim,[16] L. Kirsch,[2] K. Kondo,[16] U. Kruse,[8] S. E. Kuhlmann,[12] A. T. Laasanen,[12] W. Li,[1] T. Liss,[3] N. Lockyer,[10] F. Marchetto,[15] R. Markeloff,[17] L. A. Markosky,[17] P. McIntyre,[15] A. Menzione,[11] T. Meyer,[15] S. Mikamo,[8] M. Miller,[10] T. Mimashi,[16] S. Miscetti,[5] M. Mishina,[8] S. Miyashita,[16] N. Mondal,[17] S. Mori,[16] Y. Morita,[16] A. Mukherjee,[4] C. Newman-Holmes,[4] L. Nodulman,[1] R. Paoletti,[11] A. Para,[4] J. Patrick,[4] T. J. Phillips,[6] H. Piekarz,[2] R. Plunkett,[13] L. Pondrom,[17] J. Proudfoot,[1] G. Punzi,[11] D. Quarrie,[4] K. Ragan,[10] G. Redlinger,[3] J. Rhoades,[17] L. Ristori,[11] T. Rohaly,[10] A. Roodman,[3] A. Sansoni,[5] R. Sard,[7] V. Scarpine,[7] P. Schlabach,[7] E. E. Schmidt,[4] P. Schoessow,[1] M. H. Schub,[12] R. Schwitters,[6] A. Scribano,[11] S. Segler,[4] M. Sekiguchi,[16] P. Sestini,[11] M. Shapiro,[6] M. Sheaff,[17] M. Shibata,[16] M. Shochet,[3] J. Siegrist,[9] P. Sinervo,[10] J. Skarha,[17] D. A. Smith,[7] F. Snider,[3] R. St. Denis,[6] A. Stefanini,[11] Y. Takaiwa,[16] K. Takikawa,[16] S. Tarem,[2] D. Theriot,[4] A. Tollestrup,[4] G. Tonelli,[11] W. Trischuk,[6] Y. Tsay,[3] F. Ukegawa,[16] D. Underwood,[1] R. Vidal,[4] R. G. Wagner,[1] R. L. Wagner,[4] J. Walsh,[10] T. Watts,[14] R. Webb,[15] T. Westhusing,[7] S. White,[13] A. Wicklund,[1] H. H. Williams,[10] T. Yamanouchi,[4] A. Yamashita,[16] K. Yasuoka,[16] G. P. Yeh,[4] J. Yoh,[4] and F. Zetti[11]

[1]*Argonne National Laboratory, Argonne, Illinois 60439*
[2]*Brandeis University, Waltham, Massachusetts 02254*
[3]*University of Chicago, Chicago, Illinois 60637*
[4]*Fermi National Accelerator Laboratory, Batavia, Illinois 60510*
[5]*Laboratori Nazionale di Frascati, Instituto Nazionale di Fisica Nucleare, Frascati, Italy*
[6]*Harvard University, Cambridge, Massachusetts 02138*
[7]*University of Illinois, Urbana, Illinois 61801*
[8]*National Laboratory for High Energy Physics (KEK), Tsukuba-gun, Ibaraki-ken 305, Japan*
[9]*Lawrence Berkeley Laboratory, Berkeley, California 94720*
[10]*University of Pennsylvania, Philadelphia, Pennsylvania 19104*
[11]*Istituto Nazionale di Fisica Nucleare, University and Scuola Normale Superiore of Pisa, I-56100 Pisa, Italy*
[12]*Purdue University, West Lafayette, Indiana 47907*
[13]*Rockefeller University, New York, New York 10021*
[14]*Rutgers University, Piscataway, New Jersey 08854*
[15]*Texas A&M University, College Station, Texas 77843*
[16]*University of Tsukuba, Ibaraki 305, Japan*
[17]*University of Wisconsin, Madison, Wisconsin 53706*

(Received 23 December 1988)

The cross section for the production and subsequent decay to electron and neutrino of the W intermediate vector boson has been measured in 1.8-TeV $\bar{p}p$ collisions at the Fermilab Tevatron Collider. An analysis of events with missing transverse energy greater than 25 GeV and with an electron of transverse energy greater than 15 GeV from a datum sample of 25.3 nb^{-1} gives $\sigma B = 2.6 \pm 0.6 \pm 0.5$ nb.

PACS numbers: 13.85.Qk, 14.80.Er

© 1989 The American Physical Society

The conventional mechanism for the production of W bosons in high-energy $\bar{p}p$ collisions is the Drell-Yan process[1]—the annihilation of a quark and an antiquark into the W. The first-order cross section is directly predicted from the quark momentum distributions in the proton (structure functions) and the weak coupling constant[2]; higher-order strong-interaction corrections have also been calculated.[3] One expects an approximately threefold increase in the W-boson production cross section at the Fermilab Tevatron energy of 1.8 TeV compared to the measured results[4] at the CERN collider energy of 0.63 TeV. We report here a measurement using the Collider Detector at Fermilab of σB at 1.8 TeV, where B is the branching ratio of the W to electron and neutrino.

A brief description of the Collider Detector at Fermilab follows: The apparatus is described fully in Ref. 5. Vertex time-projection chambers around the beam pipe are used to determine the event vertex position. The central tracking chamber which surrounds the vertex time-projection chamber system and is immersed in a 1.5-T axial magnetic field, provides momentum determination of charged particles with a resolution of $\delta P_T/P_T^2 \simeq 0.002$ $(\mathrm{GeV}/c)^{-1}$.

The electromagnetic (EM) and hadronic (HAD) calorimeters are arranged in a fine-grained projective geometry covering polar angles from 2° to 178°. The calorimeters are organized into three major angular or pseudorapidity $[\eta = -\ln(\tan\theta/2)]$ regions: the "central" and "end wall" regions ($|\eta| < 1.1$); the "end-plug" ($1.1 < |\eta| < 2.4$) region; and the "forward" ($2.4 < |\eta| < 4.2$) region. The central calorimeters are scintillator based whereas the end-plug and forward calorimeters use gas proportional chambers.

The calorimeter towers are approximately 0.1 wide in η and 15° or 5° wide in azimuth (ϕ), for scintillating sampling and gas sampling calorimeters, respectively. Planes of scintillation counters on each side of the interaction point (the beam-beam counter system) cover the region $3.2 < |\eta| < 5.9$. Signals from these counters are used in the event trigger and in the luminosity monitor.

Events used in the analysis were required to have a central electron candidate ($|\eta| < 1.1$) which passed the hardware trigger requirements of (1) at least one beam-beam counter signal on both sides of the detector; (2) transverse electromagnetic energy[6] $E_T(\mathrm{EM})$ of 5 GeV or more in a "trigger tower" of $\Delta\eta \times \Delta\phi = 0.2 \times 15°$; and (3) the total $E_T(\mathrm{EM})$ exceeding a threshold which varied from 7 to 15 GeV depending on run conditions. This work is based on 4×10^5 recorded events corresponding to an integrated luminosity of 25.3 nb^{-1}.

Two separate analysis paths were followed. One focused on missing transverse energy ($\not{E}_T$) in order to identify events with a "missing" neutrino. A second path focused on the identification of isolated electrons. Both analysis paths, discussed in detail below, led to essentially the same set of W-candidate events, providing a robust cross check of the detector performance and calculated efficiencies.

We start with the $\not{E}_T$ path. $\not{E}_T$ is defined as the magnitude of the vector sum of transverse energy over all the EM and hadron cells of the calorimeter in the region $|\eta| < 3.6$. The total transverse energy (E_T) in an event is defined as the corresponding scalar sum. A total of 4178 events passed the requirement that the $\not{E}_T$ be greater than 25 GeV. A jet-clustering algorithm[7] was applied to each event, with 1604 events passing a requirement that there be at least one cluster with $E_T(\mathrm{EM}) > 15$ GeV in the detector towers within the range $|\eta| < 1$.

Further cuts were imposed to suppress sources of background peculiar to the $\not{E}_T$ sample: (1) Events triggered by cosmic rays and stray particles from the Fermilab main ring (which passes above the detector) were suppressed by requiring less than 3 GeV of energy in the central hadron calorimeter outside of a 20-ns interval centered at the beam crossing time. (2) A sensitivity to low-energy neutrons is seen in the gas hadron calorimeters as clusters with little EM energy. We defined as spurious and removed any cluster with less than 5% EM energy. Based on the study of an independent sample of jet triggers, we estimate that only $(0.03 \pm 0.03)\%$ of real clusters would be lost by this requirement. (3) Events with a cluster greater than 5 GeV within a $\Delta\phi = \pm 30°$ interval opposite to the leading cluster were eliminated (dijet cut). This cut removed QCD jet-jet events in which mismeasurement of the energy of a jet induced a large value of $\not{E}_T$ along the jet direction. (4) Overall fluctuations in $\not{E}_T$ measurements contribute to background. Studies of "minimum-bias events" show that in a projection on any given axis $\not{E}_T$ has a Gaussian distribution with an rms deviation of $\sigma = 0.7\sqrt{E_{T'}}$, where all energies are expressed in GeV. Here $E_{T'}$ is the total scalar transverse energy observed within $|\eta| < 2.4$. Events were required to have $\not{E}_T > 2.8\sqrt{E_{T'}}$, a value determined from a sample of jet events to ensure a clear separation of jet-induced background.

Of the 115 events which passed the above criteria, 22 have electrons based on very loose cuts: one track with momentum P pointing to a cluster with energy E such that $E/P < 2$ and $E_{\mathrm{EM}}/(E_{\mathrm{EM}} + E_{\mathrm{HAD}}) > 0.85$. A scan of the 115 events shows there is none in which a track has been missed. The remaining events include one event which has a 9-GeV/c track pointing toward a 30-GeV cluster, consistent with a real $W \to e\nu$ plus bremsstrahlung. A theoretical calculation[8] predicts that $(3 \pm 1)\%$ of the electrons from W decay radiate more than 50% of their energy, and hence would fail the $E/P < 2$ cut. Most of the remaining nonelectron events in the $\not{E}_T$ sample are residual cosmic rays, main ring background, "coherent" electronic calorimeter noise, mismeasured

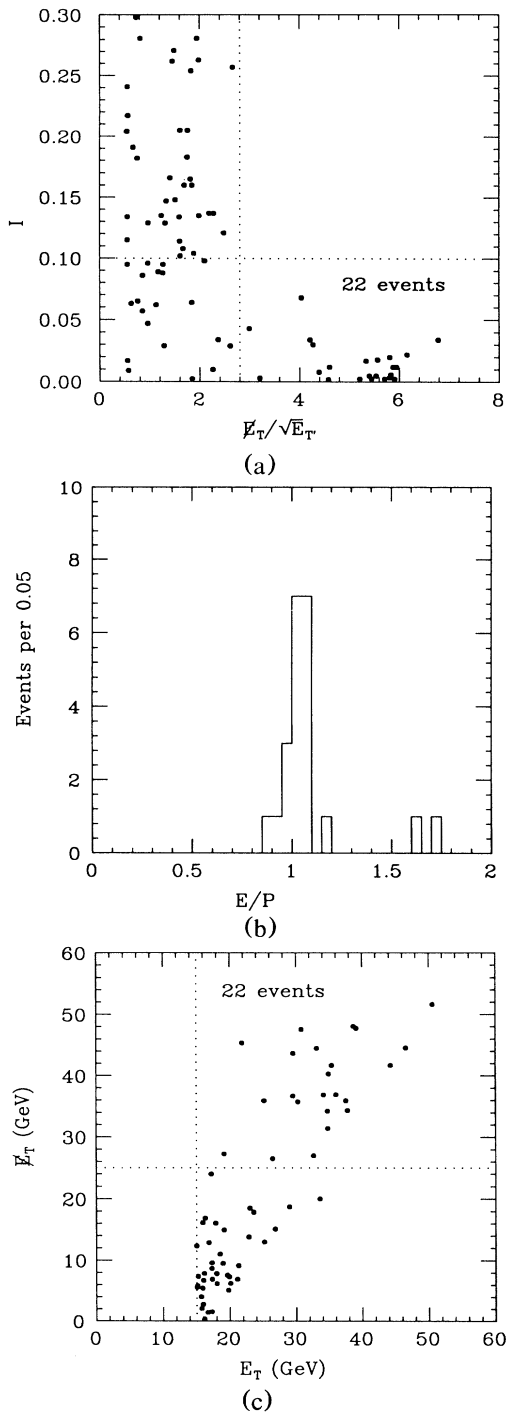

FIG. 1. (a) The distribution of events in isolation I vs $\not{E}_T/\sqrt{E_{T'}}$ where $\not{E}_T$ and $E_{T'}$ are in GeV. The sample contains events which satisfy all electron cuts except the isolation and $\not{E}_T$ cuts. Events with $I > 0.3$ are not shown. The dotted lines indicate the final cuts. (b) The distribution of E/P for the 22 W candidates. (c) The distribution of $\not{E}_T$ vs E_T for the 61 events in the "electron" analysis path before the final $\not{E}_T$ cut. The horizontal dotted line indicates where the $\not{E}_T$ cut was imposed.

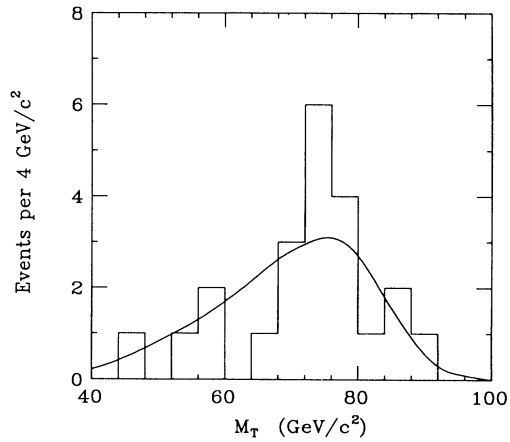

FIG. 2. The distribution in transverse mass for the W candidate events. The curve is an ISAJET (Ref. 10) prediction for a W mass of 80 GeV/c^2.

calorimeter energy identified by a large mismatch with the momenta as measured by the tracking chambers, or measurement fluctuations of multiple jet events.

We now describe a parallel W search based on the identification of electrons. Events were selected by requiring an isolated, central EM cluster ($|\eta| < 1.0$) with $E_T > 15$ GeV. The hadronic-to-EM ratio of the energy in the cluster was required to be less than 0.05, a value determined from test beam data to be 96% efficient for electrons. If E_C is taken to be the total transverse electron within a cone of radius $R = (\Delta\eta^2 + \Delta\phi^2)^{1/2} = 0.4$ centered on the electron cluster, we define a measure of isolation by $I = (E_C - E_T)/E_T$. An isolation cut required $I < 0.1$. A total of 3753 events satisfied these criteria.

The jet background was reduced by requiring at least one track with momentum P pointing at the cluster such that $E/P < 2$. There are 138 events which passed this cut. Six of these have a second EM cluster with a high invariant mass for the pair and are considered $Z \rightarrow e^+e^-$ candidates. The remaining background is dominated by QCD jet events where one jet fakes an electron. To reduce this background, a dijet cut was applied which removed events having a cluster with $E_T > 5$ GeV opposite ($\pm 30°$ in ϕ) the electron candidate, leaving 62 events. A requirement that $\not{E}_T > 25$ GeV reduced the sample to 22 $W \rightarrow e\nu$ candidates, the same 22 found by the $\not{E}_T$ analysis path.

Sample distributions relevant to the analyses are shown in Fig. 1. The distribution in transverse mass $M_T = [2E_T^e E_T^\nu (1 - \cos\Delta\phi_{e\nu})]^{1/2}$ is shown in Fig. 2. A fit of the expected spectrum gives $M_W = 80.0 \pm 3.3 \pm 2.4$ GeV/c^2, where the first error is statistical and the second is systematic. The systematic error is dominated by the uncertainty in the absolute energy scale.

The cross section and its estimated uncertainty are determined by using the 22 events corrected for

TABLE I. Background and efficiency values for the $\not{E}_T$ and electron analysis paths. The $\not{E}_T$ and E_T cuts are included in "Thresholds," as is an electronic trigger efficiency of 99.7%.

	$\not{E}_T$	Electron
	Background (events)	
$W \to \tau\nu_\tau$	0.6 ± 0.1	
Top	< 0.2	
QCD jet	<0.2	0.6 ± 0.3
	Selection efficiencies	
$\lvert\eta\rvert < 1.0$	0.50 ± 0.05	
Detector gaps	0.91 ± 0.01	
Thresholds	0.84 ± 0.02	
Dijet cut	0.91 ± 0.02	
Radiative corrections	0.97 ± 0.01	
Tracking	···	0.98 ± 0.02
HAD/EM	···	0.96 ± 0.04
Isolation	···	0.99 ± 0.01
Timing	0.99 ± 0.01	···
Total	0.33 ± 0.04	0.31 ± 0.04

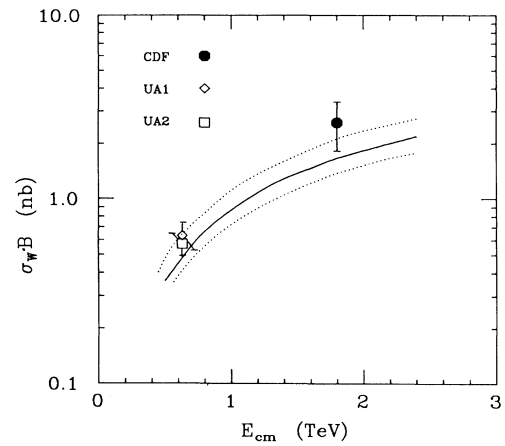

FIG. 3. The cross section times branching ratio for $W \to e\nu$ vs c.m. energy. The prediction is from Ref. 3, adjusted for a W mass of 80 GeV/c^2. The dotted lines indicate the 1σ error limits for the theoretical curve.

efficiency and background. Efficiency and background estimates for the two analysis paths are shown in Table I. Three potential types of background to $W \to e\nu$ are the sequential decay $W \to \tau\nu_\tau \to e\nu X$, jet events with one jet faking an electron, and possibly a top quark directly producing a high-E_T isolated electron. The jet background was calculated from the data while the other two types were estimated from Monte Carlo studies.

Efficiency losses resulting from the electron rapidity cut, thresholds, and gaps between calorimeter modules (fiducial cuts) were calculated by Monte Carlo studies. The electron rapidity cut is the largest source of systematic error due to uncertainties in the structure functions. All other efficiencies were found directly from data.

The luminosity is based on information from the beam-beam counters. We have estimated the cross section seen by these counters as 44 ± 6 mb by extrapolating from lower energy measurements.[9]

We obtain $\sigma B(W \to e\nu) = 2.6 \pm 0.6 \pm 0.5$ nb. This result is shown along with previous measurements in Fig. 3. The expected increase in W production is observed.

This work would not have been possible without the skill and hard work of the Accelerator Division of Fermilab. We thank the staffs of our institutions for their many contributions to the construction of the detector. This work was supported by the U.S. Department of Energy, the National Science Foundation, the Istituto Nazionale di Fisica Nucleare, the Ministry of Science, Culture, and Education of Japan, and the A. P. Sloan Foundation.

[1]Y. Yamaguchi, Il Nuovo Cimento **43A**, 193 (1966); S. D. Drell and T-M. Yan, Phys. Rev. Lett. **25**, 316 (1970).

[2]L. M. Lederman and B. G. Pope, Phys. Rev. Lett. **27**, 765 (1971); R. B. Palmer, E. A. Paschos, N. P. Samios, and Ling-Lie Wang, Phys. Rev. D **14**, 118 (1976); C. Quigg, Rev. Mod. Phys. **49**, 297 (1977).

[3]G. Altarelli, K. Ellis, M. Greco, and G. Martinelli, Nucl. Phys. **B246**, 12 (1984); G. Altarelli, K. Ellis, and G. Martinelli, Z. Phys. C **27**, 617 (1985).

[4]C. Albajar *et al.*, Phys. Lett. B **198**, 271 (1987); G. Arnison *et al.*, Phys. Lett. **122B**, 103 (1983); M. Banner *et al.*, Phys. Lett. **122B**, 476 (1983).

[5]F. Abe *et al.*, Nucl. Instrum. Methods A **271**, 387 (1988).

[6]The transverse energy of a tower is the energy in the tower multiplied by $\sin\theta$ of the tower.

[7]See S. Kim, in *Proceedings of Physics in Collision VII, Tsukuba, Japan, 1987,* edited by T. Kondo and K. Takahashi (World Scientific, London, 1987), p. 185.

[8]The radiative correction was calculated with an algorithm similar to that of F. A. Berends *et al.*, Z. Phys. C **27**, 155 (1985).

[9]M. Bozzo *et al.*, Phys. Lett. **147B**, 392 (1984); R. E. Ansorge *et al.*, Z. Phys. C **33**, 175 (1987); G. J. Alner *et al.*, Z. Phys. C **32**, 153 (1987).

[10]F. Paige and S. D. Protopopescu, BNL Report No. BNL 38034, 1986 (unpublished). We thank E. Berger, S. Ellis, and J. Rosner for discussions and for help in investigating other choices of structure functions.